4.4 Lift Due to Combined Wing-Fuselage-Nacelle

The addition of a body to a wing results in mutual interference effects. Lift of the wing-body combination is influenced by the body upwash effect on wing lift and the lift carryover of wing panel loading onto the body. Net wing upwash and downwash effects on the body influence body pitching moments primarily. Symmetrical body vortices which result from flow separation just behind or above the area of minimum pressure along the side of the body near the nose are normally negligible for most airplane types of wing-body combinations.

The lift of the wing-fuselage-nacelle combination accounting for the mutual interference effects of wing and fuselage may be estimated from

$$C_{L_{wfn}} = C_{L_f} + C_{L_n} + \left[K_{w(f)} + K_{f(w)}\right] \left(C_{L_\alpha}\right)_{w_e} \alpha_{w_{abs}} \frac{S_{w_e}}{S_w} \qquad (4.4\text{-}1)$$

where

C_{L_f} is the fuselage lift from equation (4.3-3)

C_{L_n} is the nacelle lift from equation (4.3-3)

$K_{w(f)}$ is the ratio of the lift on the wing in the presence of the body to the lift on an isolated wing, obtained from figure 4.4-1 and reference 11

$K_{f(w)}$ is the ratio of wing lift carryover onto the body to wing lift alone, obtained from figure 4.4-1

$\left(C_{L_\alpha}\right)_{w_e}$ is the lift-curve slope of the exposed wing panels, obtained from table 4.2-1

$\alpha_{w_{abs}}$ is the absolute angle of attack of the wing, equal to $\alpha + i_w - \alpha_{o_w}$

Because of the lack of suitable data, the interference effects of the nacelles are not accounted for.

The use of the interference factors, $K_{w(f)}$ and $K_{f(w)}$, from reference 11 is restricted to wings which do not have sweptback trailing edges or sweptforward leading edges. The factors were obtained for wings mounted as midwings on bodies of revolution but have been used for other configurations.

For the subject airplane, the lift of the wing in the presence of the body and the carryover of the wing lift onto the body is calculated in table 4.4-1(a) to be equal to

$$C_{L_{w(f)+f(w)}} = 0.079(\alpha + 4) \text{(referenced to } S_w = 172.3 \text{ sq ft)} \qquad (4.4\text{-}2)$$

The net lift of the wing, fuselage, and nacelle combination in the linear lift range is obtained by summarizing the fuselage and nacelle contributions as obtained from table 4.3-1 and the lift of the wing in the presence of the body as obtained from table 4.4-1(a). Thus

$$C_{L_{wfn}} = C_{L_f} + C_{L_n} + C_{L_{w(f)+f(w)}}$$

$$= [0.00218(\alpha - 3) + 0.0000309(\alpha - 3)^2] + [0.00160\alpha + 0.000010\alpha^2] + 0.079(\alpha + 4) \tag{4.4-3}$$

The addition of a body to the wing in most airplane configurations tends to decrease the maximum lift coefficient and corresponding angle of attack, although an increase in the geometric stall angle is possible in some circumstances. The wing planform is a primary consideration. In the absence of theoretical methods, reference 1 devised empirical relations for predicting maximum lift coefficient, $(C_{L_{max}})_{wf}$, and corresponding stall angle, $(\alpha C_{L_{max}})_{wf}$, for wing-body combinations up to M = 0.6. The method uses an empirical taper ratio correction factor, c_2 (fig. 4.4-2), in determining, in the following equations, the empirical correction factors, $\frac{(C_{L_{max}})_{wf}}{(C_{L_{max}})_w}$ and $\frac{(\alpha C_{L_{max}})_{wf}}{(\alpha C_{L_{max}})_w}$, from figure 4.4-3 as functions of $(c_2 + 1)A \tan \Lambda_{le}$ and the ratio of the fuselage diameter to the wing span, $\frac{d}{b}$:

$$(C_{L_{max}})_{wf} = \left[\frac{(C_{L_{max}})_{wf}}{(C_{L_{max}})_w}\right](C_{L_{max}})_w \tag{4.4-4}$$

and

$$(\alpha C_{L_{max}})_{wf} = \left[\frac{(\alpha C_{L_{max}})_{wf}}{(\alpha C_{L_{max}})_w}\right](\alpha C_{L_{max}})_w \tag{4.4-5}$$

where

$(C_{L_{max}})_w$ and $(\alpha C_{L_{max}})_w$ (the absolute stall angle from zero lift) are for total wing alone from section 4.2

Pertinent aspects of the calculations for $(C_{L_{max}})_{wf}$ and $(\alpha C_{L_{max}})_{wf}$ for the subject airplane are listed in table 4.4-1(b).

The net lift of the wing-fuselage-nacelle combination for the subject airplane in terms of a reference wing area of 172.3 square feet (reference area of analysis) and

178.0 square feet (reference area of wind-tunnel data) is summarized in table 4.4-2. The results for a wing area of 178.0 square feet are plotted and compared with wind-tunnel data in figure 4.4-4. The fairing from the limit of linearity to the maximum lift coefficient was performed in the same manner as for the wing alone (section 4.2).

In summary, the lift contributions attributed to the fuselage and nacelle crossflow effects are insignificant. The contributions due to the potential-flow effects on the fuselage and nacelles are negligible for preliminary estimates but are large enough to be significant for refined estimates. Although these fuselage contributions may be negligible or small for lift considerations, they are not necessarily negligible with regard to pitching-moment considerations, as discussed in section 4.8.

4.4.1 Symbols

A	wing aspect ratio
b	wing span, ft
C_{L_f}	lift coefficient of the fuselage based on the wing area
$\left(C_{L_{max}}\right)_w$	maximum lift coefficient of the wing alone, obtained from table 4.2-1
$\left(C_{L_{max}}\right)_{wf}$	maximum lift coefficient of the wing-fuselage combination, obtained from figure 4.4-3
C_{L_n}	lift coefficient of the nacelles based on wing area
$C_{L_{w(f)+f(w)}}$	lift coefficient of the wing including mutual wing-fuselage interference effects
$C_{L_{wfn}}$	lift coefficient of the wing-fuselage-nacelle assembly
$\left(C_{L_\alpha}\right)_{w_e}$	lift-curve slope of the exposed wing panels, obtained from table 4.2-1, per deg
c_2	taper ratio correction factor from figure 4.4-2
d	fuselage width at the wing, ft
i_w	wing incidence, angle between the wing chord and reference X-body axis, deg
$K_{f(w)}$	ratio of wing lift carryover on the fuselage to the wing alone, obtained from figure 4.4-1
$K_{w(f)}$	ratio of the lift on the wing in the presence of the fuselage to the wing alone, obtained from figure 4.4-1
M	Mach number

S_w	reference wing area, sq ft
S_{w_e}	area of the exposed wing panels, sq ft
α	angle of attack relative to the reference X-body axis, deg
$\left(\alpha_{C_{L_{max}}}\right)_w$	stall angle of attack of the wing alone relative to the zero-lift line of the wing, deg
$\left(\alpha_{C_{L_{max}}}\right)_{wf}$	stall angle of attack of the wing-fuselage combination relative to the zero-lift line of wing, deg
α_{o_w}	wing zero-lift angle of attack relative to the wing chord, deg
$\alpha_{w_{abs}}$	wing angle of attack relative to the wing zero-lift line, $\alpha - \alpha_{o_w} + i_w$, deg
Λ_{le}	sweep of the wing leading edge, deg
λ	wing taper ratio

TABLE 4.4-1

WING LIFT OF AIRPLANE INCLUDING MUTUAL WING-FUSELAGE INTERFERENCE

(a) In linear range

$$C_{L_{w(f)+f(w)}} = \left[K_{w(f)} + K_{f(w)}\right]\left(C_{L_\alpha}\right)_{w_e} \alpha_{w_{abs}} \frac{S_{w_e}}{S_w}$$

Symbol	Description	Reference	Magnitude
d	Fuselage width at wing, ft	Figure 3.2-1	4.0
b	Wing span, ft	Figure 3.2-1	36.0
S_w	Reference wing area, sq ft	Table 3.2-1	172.3
S_{w_e}	Area of exposed wing panels, sq ft	Table 3.2-1	148.0
α_{o_w}	Zero-lift angle of attack relative to wing chord, deg	Table 4.2-1	-2.0
i_w	Wing incidence relative to X-body axis, deg	Table 3-1	2.0
$\alpha_{w_{abs}}$	Wing angle of attack relative to zero lift, $\alpha - \alpha_{o_w} + i_w$, deg	----------	$\alpha + 4$
$\left(C_{L_\alpha}\right)_{w_e}$	Lift-curve slope of exposed wing panels per deg	Table 4.2-1	.0747
$\frac{d}{b}$	Fuselage-width to wing-span ratio	----------	0.111
$K_{w(f)}$	Ratio of lift on wing in presence of fuselage to wing alone	Figure 4.4-1	1.09
$K_{f(w)}$	Ratio of wing lift carryover on fuselage to wing alone	Figure 4.4-1	.14
Summary: $C_{L_{w(f)+f(w)}} = 0.079(\alpha + 4)$			

(b) Maximum lift of wing with mutual wing-body interference

$$\left(C_{L_{max}}\right)_{wf} = \left[\frac{\left(C_{L_{max}}\right)_{wf}}{\left(C_{L_{max}}\right)_w}\right]\left(C_{L_{max}}\right)_w ; \left(\alpha C_{L_{max}}\right)_{wf} = \left[\frac{\left(\alpha C_{L_{max}}\right)_{wf}}{\left(\alpha C_{L_{max}}\right)_w}\right]\left(\alpha C_{L_{max}}\right)_w$$

Symbol	Description	Reference	Magnitude
λ	Wing taper ratio	Table 3.2-1	0.513
c_2	Taper ratio correction factor	Figure 4.4-2	.103
Λ_{le}	Leading-edge sweep of wing, deg	Table 3.2-1	0
A	Wing aspect ratio	Table 3.2-1	7.5
$(c_2 + 1)A \tan \Lambda_{le}$	----------	----------	0
$\frac{d}{b}$	----------	----------	.111
$\left[\frac{\left(C_{L_{max}}\right)_{wf}}{\left(C_{L_{max}}\right)_w}\right]$	Ratio of $C_{L_{max}}$ of wing-fuselage to wing alone	Figure 4.4-3	1.0
$\left[\frac{\left(\alpha C_{L_{max}}\right)_{wf}}{\left(\alpha C_{L_{max}}\right)_w}\right]$	Ratio of stall angle of wing-fuselage to wing alone	Figure 4.4-3	1.025
$\left(C_{L_{max}}\right)_w$	Maximum lift coefficient of wing alone	Table 4.2-1	1.23
$\left(\alpha C_{L_{max}}\right)_w$	Stall angle of wing alone relative to zero lift, deg	Table 4.2-1	15.5 + 2 = 17.5
Summary: $\left(C_{L_{max}}\right)_{wf} = 1.23$; $\left(\alpha C_{L_{max}}\right)_{wf} = 17.8$			

TABLE 4.4-2

SUMMARY OF WING-FUSELAGE-NACELLE LIFT

$$C_{L_{wfn}} = [0.00218(\alpha - 3) + 0.0000309(\alpha - 3)^2] + [0.00160\alpha + 0.000010\alpha^2] + 0.079(\alpha + 4)$$

①	②	③	④	⑤	⑥	⑦	⑧	⑨
α relative to body X-axis, deg	$\alpha_{w_{abs}}$ relative to wing zero lift = α+4, deg	C_{L_f} (eq. (4.4-3) based on S_w = 172.3 sq ft)		C_{L_n} (eq. (4.4-3) based on S_w = 172.3 sq ft)		$\left[K_{w(f)} + K_{f(w)}\right]\left(C_{L_\alpha}\right)_{w_e} \alpha_{w_{abs}} \frac{S_{w_e}}{S_w}$ = 0.079 ② (eq. (4.4-2) based on S_w = 172.3 sq ft)	$C_{L_{wfn}}$ = ③ + ④ + ⑤ + ⑥ + ⑦ on basis of S_w = 172.3 sq ft	$C_{L_{wfn}}$ = 0.968 ⑧ on basis of S_w = 178 sq ft
		Potential flow = 0.00218 (① - 3.0)	Crossflow = 0.000031 (① - 3.0)^2	Potential flow = 0.00160 ①	Crossflow = 0.000010 ①^2			
-4	0	-0.01526	0.00152	-0.00640	0.00016	0	-0.01998	-0.0194
-2	2	-.01090	.000775	-.00320	.00004	.158	.147	.140
0	4	-.00654	.000279	0	0	.316	.310	.300
2	6	-.00218	.000031	.00320	.00004	.474	.475	.460
4	8	.00218	.000031	.00640	.00016	.632	.641	.620
6	10	.00654	.000279	.00960	.00036	.790	.807	.781
8	12	.01090	.000775	.01280	.00064	.949	.973	.942
10	14	.01526	.00152	.01600	.00100	1.106	1.140	1.104
12	16	.01962	.00251	.01920	.00144	-----(nonlinear range)	-----	-----
13.8	[a]17.8	.02354	.00366	.02210	.00190	[a]1.23	1.281	[b]1.280

[a] $\left(\alpha C_{L_{max}}\right)_{wf}$ = 17.8° relative to zero-lift line of wing (table 4.4-1(b)); $C_{L_{max}}$ of wing with mutual wing-body interference = 1.23 (table 4.4-1(b)).

[b] $\left(C_{L_{max}}\right)_{wfn}$ on basis of (S_w = 178 sq ft) = $\left[C_{L_f} + C_{L_n}\right]\left(\frac{S_w = 172.3}{S_w = 178.0}\right) + \left[C_{L_{max}}\text{ in column ⑦}\right]$.

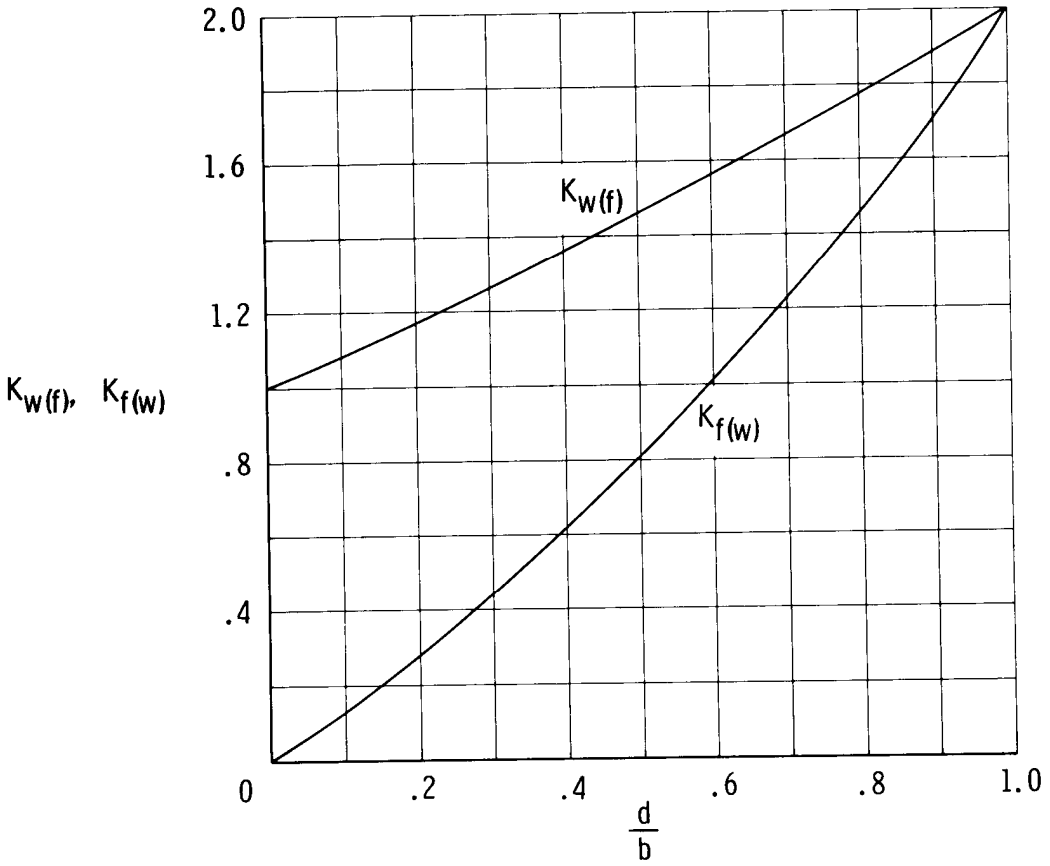

Figure 4.4-1. Lift ratios $K_{w(f)}$ and $K_{f(w)}$ based on slender-body theory with the wing at fixed incidence relative to the fuselage (ref. 11). Applicable at all speeds.

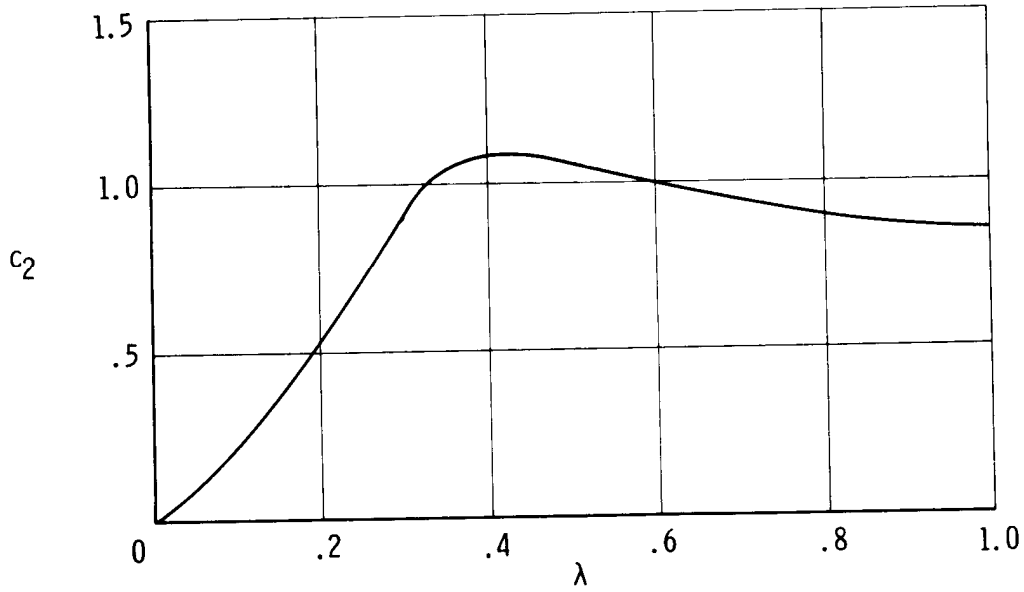

Figure 4.4-2. Taper ratio correction factors (ref. 1).

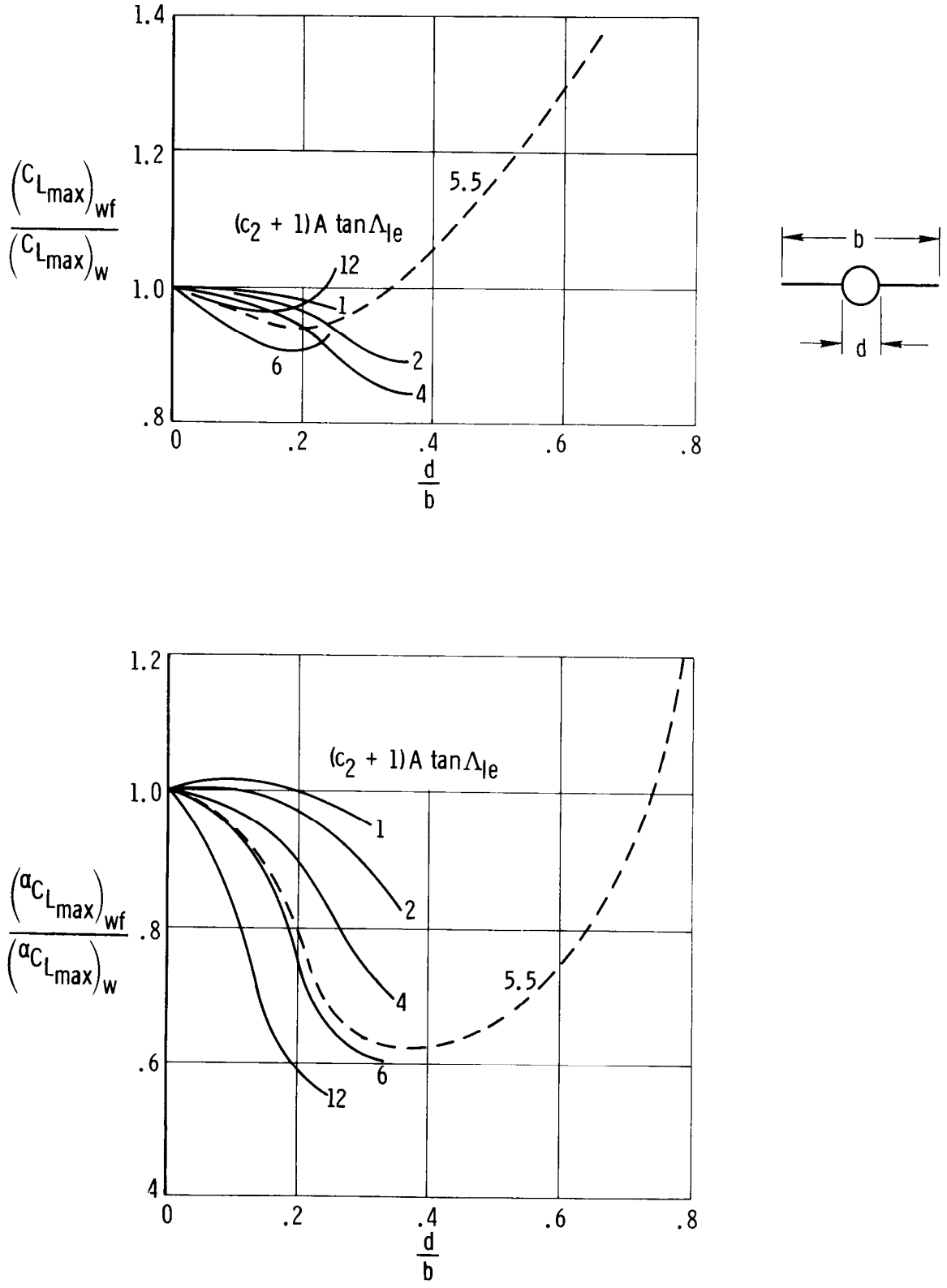

Figure 4.4-3. Wing-body maximum lift and angle of attack for maximum lift below M = 0.6 (ref. 1).

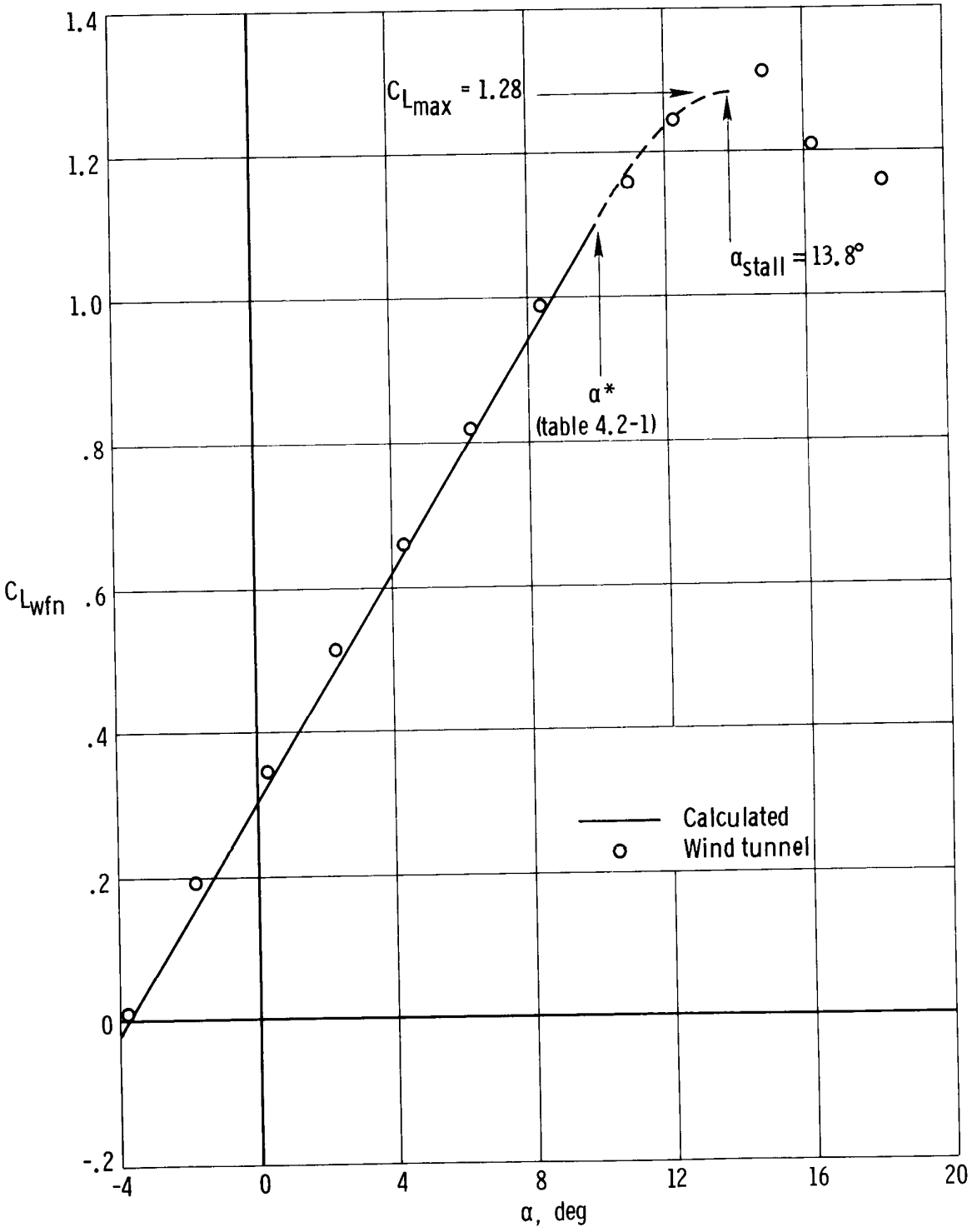

Figure 4.4-4. Comparison of predicted wing-fuselage-nacelle lift curve with wind-tunnel data. S_w = 178 sq ft.